



Synthesis and Multifunctional Characterization of Multiferroic BZT-BFO Nanocomposites for Biomedical Devices

Anupamaa Shankara Narayanan*

Scientist, Quality and Regulatory Department, AMTZ.

Received: 22nd October, 2025; Revised: 15th November, 2025; Accepted: 26th November, 2025; Available Online: 08th December, 2025

ABSTRACT

Background: Nanocomposites based on multiferroic barium zirconate titanate (BZT) and bismuth ferrite (BFO) present simultaneous ferroelectric and magnetic ordering, desirable for next-generation devices.[1]

Methods: BZT, BFO, and composite BZTBFO powders were synthesized by 12-hour high-energy ball milling of stoichiometric precursors, followed by sintering at 1400°C (BZT), 800°C (BFO), and 700°C (BZTBFO). Characterization included X-ray diffraction (XRD), scanning electron microscopy (SEM), thermogravimetric/differential thermal analysis (TG/DTA), density measurement, AC impedance spectroscopy, and vibrating sample magnetometry (VSM).

Results: XRD confirmed pure tetragonal phase in BZT (~57 nm crystallite size), orthorhombic/anorthic phase in BFO (~60 nm), and mixed phase BZTBFO with significantly reduced size (~27 nm). SEM revealed dense, uniform nanostructures for BZTBFO versus grain boundary fragmentation in BFO. TG/DTA showed thermal stability beyond 800 °C. Relative densities reached ~93% (BZT), 86% (BFO), and 92% (composite). Impedance measurements indicated the lowest resistance (~2.5 Ω) for BZT; the composite exhibited $R \approx 9 \Omega$. VSM showed the highest remanent polarization ($P_r = 142 \mu\text{C}/\text{mm}^2$) and lowest coercivity ($E_c = 0.71 \text{ kV}/\text{cm}$) for BZTBFO.

Conclusion: BZTBFO nanocomposite demonstrates enhanced structural, thermal, dielectric, and ferroelectric properties, highlighting its potential for multiferroic applications.[3]

Keywords: BZT; BFO; Nanocomposite; XRD; SEM; TG/DTA; Ferroelectricity
International Journal of Health Technology and Innovation (2025)

How to cite this article: Narayanan AS. Synthesis and Multifunctional Characterization of Multiferroic BZT-BFO Nanocomposites for Biomedical Devices. International Journal of Health Technology and Innovation. 2025;4(3):31-35.

Doi: 10.60142/ijhti.v4i03.05

Source of support: Nil.

Conflict of interest: None

INTRODUCTION

Multiferroic materials providing both ferroelectric and magnetic ordering are technologically significant for memory, sensing, and actuator applications. [1,5] Barium titanate (BaTiO_3) doped with zirconium (BZT) exhibits ferroelectric behavior near room temperature[2], while bismuth ferrite (BFO) presents magnetic-ferroelectric coupling[4]. Combining these into a composite (BZTBFO) may synergistically yield enhanced multifunctional performance[3]. This study aims to synthesize and systematically characterize these nanocomposites, addressing research gaps in achieving reduced crystallite size, high density, thermal stability, and low coercivity at relatively low sintering temperatures.

MATERIALS AND METHODS

Note: Measurements repeated in triplicate; uncertainties $\pm 3\text{--}5\%$.

Synthesis

Stoichiometric mixtures of BaCO_3 , ZrO_2 , TiO_2 (for BZT), Bi_2O_3 and Fe_2O_3 (for BFO), and their blends for composite ($\text{BZT}_{0.75}\text{--BFO}_{0.25}$) were milled under Toluene using zirconia balls at 1:10 ball-to-powder ratios, at 350 rpm for 12 hours in a ball mill. Powders were washed, dried overnight, and sintered: BZT at 1400°C, BFO at 800°C, BZTBFO at 700°C, each for 2 hours.[8]

Characterization

- XRD: Rigaku Miniflux IIC with $\text{Cu K}\alpha$ radiation, 2θ range 20–80°, step 2°/min. Crystallite size via Scherrer formula.
- SEM: Gold-coated samples under vacuum ≈ 0.01 Torr.
- TG/DTA: Heating rate 5 °C/min up to ~1000 °C under N_2 .
- Density: Archimedes' method; samples boiled in water 5–8 h.
- AC impedance: Complex impedance spectrum measured across a frequency sweep.[3]

*Author for Correspondence: anupamaasivasubramanian@gmail.com

- VSM: Hysteresis (P–E) loop measurements after pellet pressing. [2]

RESULTS AND DISCUSSION

XRD Analysis

XRD for BZT indicates a pure tetragonal perovskite phase with the strongest (110) peak at 31.52° , confirming the JCPDS #898213 match. Secondary reflections correspond to (100), (111), (200), and (211). Scherrer analysis yields a crystallite size of ~ 57 nm. Lattice constants: $a = b = 4.018$ Å, $c = 4.008$ Å indicate slight tetragonality (Fig 1 and Table 1).[2,7]

For BFO, dominant (121) reflection at 23.88° and additional peaks align with JCPDS #741098. Crystallite size is ~ 60 nm. Lattice parameters ($a = 7.950$ Å, $b = 8.428$ Å, $c = 6.005$ Å) reflect orthorhombic distortion.[4]

The BZTBFO composite shows characteristic peaks of both phases. Crystallite size reduces to ~ 27 nm, attributed to structural strain and phase interaction. Mixed tetragonal/orthorhombic symmetry is evident.[3]

SEM Morphology

BZT shows well-distributed nanoparticles predominantly within the nanoscale, with sparse submicron grains (Fig. 2A). BFO micrographs exhibit a granular structure with grain boundary fragmentation due to volatility during sintering (Fig. 2B)

[4]. BZTBFO displays uniform dense nanostructure with close packing and no visible porosity (Fig. 2C), correlating with high density.[3,6]

TGDTA Thermal Behavior

For BZT, total weight loss is $\sim 13\%$ (hydroxide decomposition 35 – 190°C , oxidation 220 – 370°C with DTA peak at 355°C , carbonate breakdown 512 – 803°C); stabilization occurs beyond 800°C (Fig. 3A)[7]. BFO loses $\sim 3.5\%$ mass (32 – 187°C and 292 – 405°C oxidation peaks, crystallization at 830 – 921°C), then stable (Fig. 3B)[4]. BZTBFO exhibits two-stage mass loss: 302 – 411°C (organic decomposition) and 456 – 980°C (crystallization) with stabilization afterward (Fig. 3C)[3,6].

Density Measurements

High densities in BZT and BZTBFO reflect effective sintering and compact microstructure even at different sintering temperatures Table 2. [7,8].

AC Impedance Spectroscopy

Nyquist plots (Fig. 4) show linear behavior, indicating grain interior dominates. Resistances: BZT ~ 2.5 Ω, BFO ~ 5 Ω, BZTBFO ~ 9 Ω. Lower resistance indicates enhanced electrical conductivity in BZT, while the composite shows higher impedance due to interfacial effects.[3]

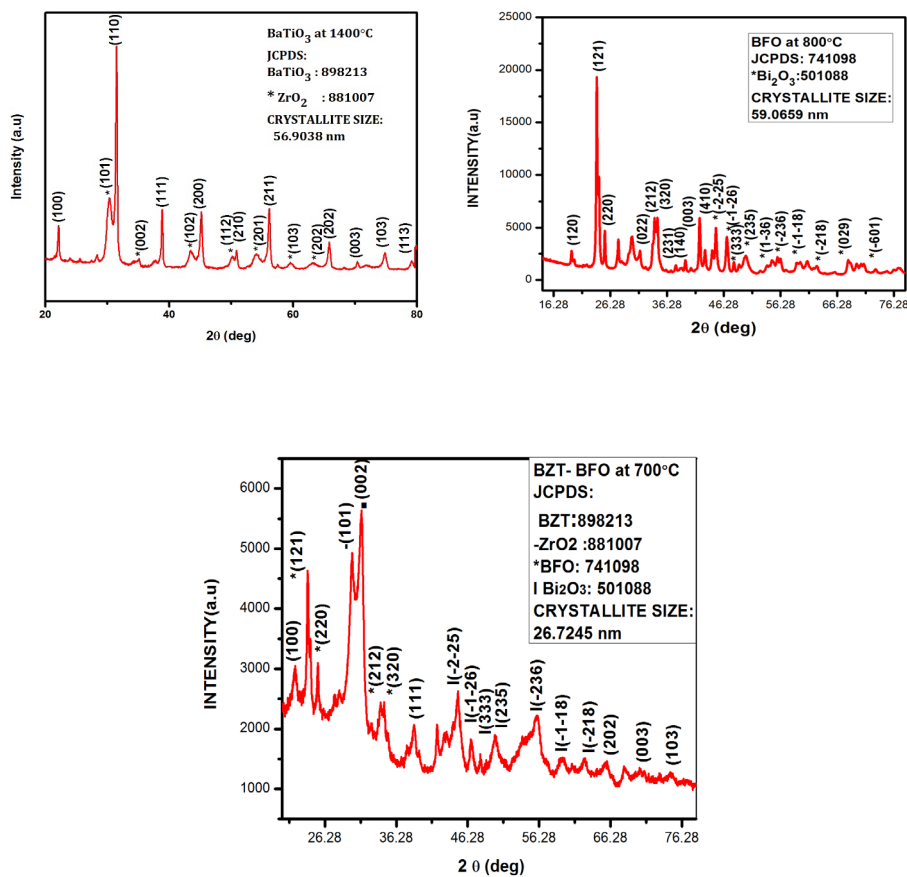


Figure 1(a, b & c): XRD patterns of BZT, BFO, and BZTBFO nanocomposites calculated using Scherrer's formula

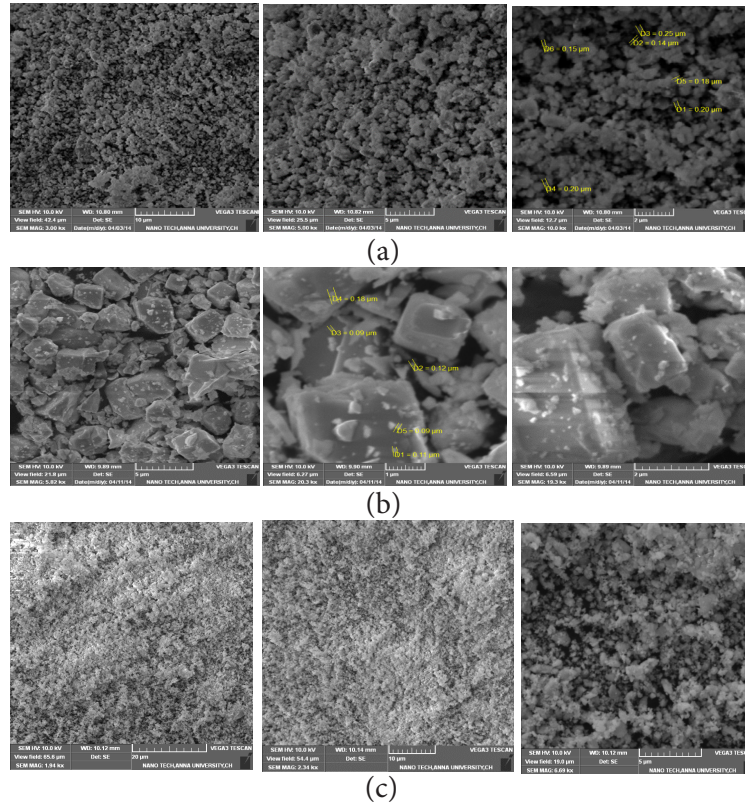


Figure 2: SEM micrographs of (A) BZT; (B) BFO; (C) BZTBFO nanocomposites at various magnifications

Table 1: Lattice parameters and crystallite sizes of synthesized nanocomposites found from XRD Characterization

<i>BZT-BFO Nanocomposites</i>	
Crystal system	Tetragonal, Orthorhombic, Anorthic
Space group	Primitive: $P_4/mmm(123)$, $P_{42}/nm(137)$, $P_{bam}(55)$, $P-1_{(2)}$
Lattice Parameters (\AA) & Angles (Deg)	$a=b=4.018$, $c=4.008(\text{BT})$ $a=b=3.598$, $c=5.512(*\text{Zr})$ $a=7.950$, $b=8.428$, $c=6.005(\text{BFO})$ $a=7.268$, $b=8.639$, $c=11.969(\text{BiO})$ & $\alpha=\beta=\gamma=90^\circ (\text{BT}) (*\text{Zr})$ $\alpha=\beta=\gamma (\text{BFO})$ $\alpha=87.713$, $\beta=93.227$, $\gamma=86.653 (\text{BiO})$

Table 2: Bulk and relative densities of synthesized samples after TG-DTA

Composite	Bulk density (g/cm^3)	Relative density (%)
BZT	5.72	93
BFO	7.30	86
BZTBFO	6.19	92

VSM Characterization

P-E hysteresis loops (Fig. 5) reveal: BZT exhibits paramagnetic-like response[2]; BFO shows $P_{\text{max}} = 139.6 \mu\text{C/mm}^2$, $P_r = 9.8 \mu\text{C/mm}^2$, $E_c = 6.3 \text{ kV/cm}$ [5]; BZTBFO demonstrates enhanced remanent polarization $P_r = 142 \mu\text{C/mm}^2$ and low coercivity $E_c = 0.71 \text{ kV/cm}$ [3]. The composite's soft switching suggests suitability for low-power functional devices.

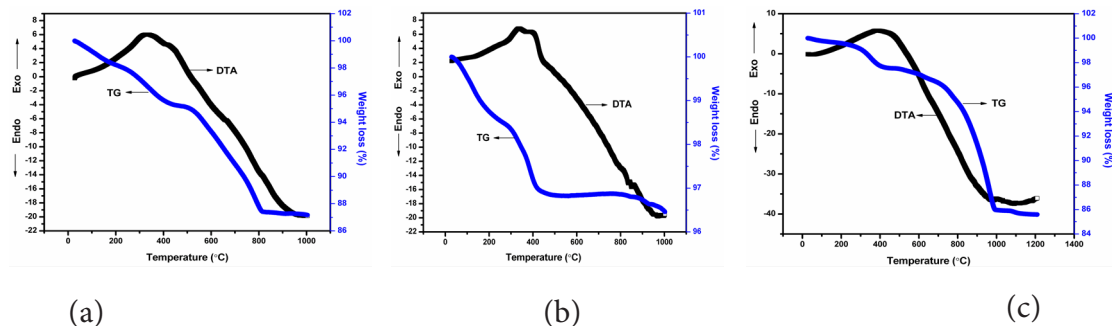


Figure 3: TGDTA curves for (A) BZT, (B) BFO, and (C) BZTBFO nanocomposites.

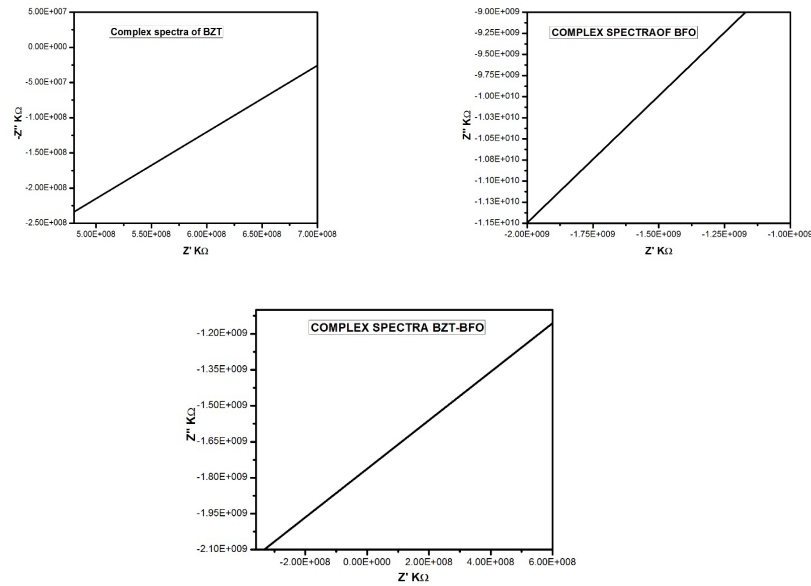


Figure 4: AC impedance spectra comparing BZT, BFO, and BZTBFO nanocomposites

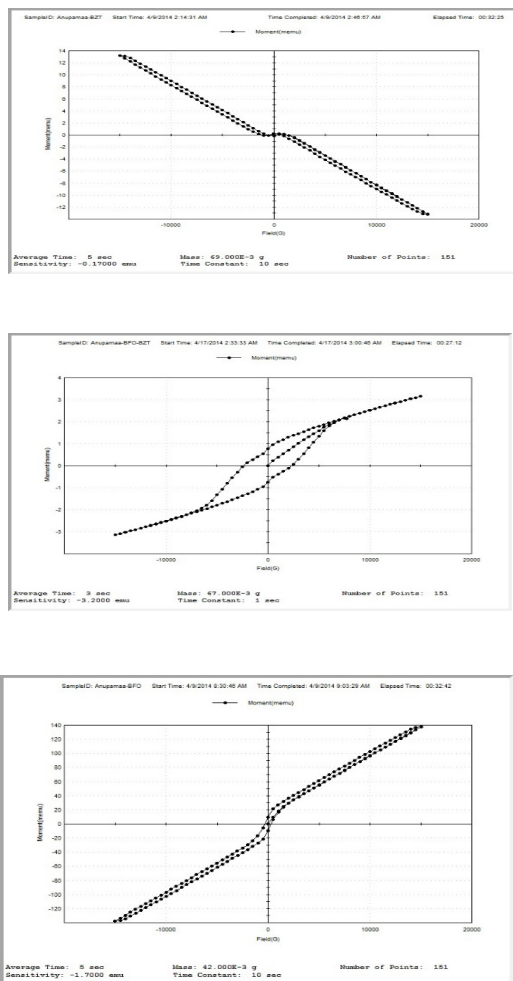


Figure 5: P-E hysteresis loops for BZT, BFO, and BZT BFO nanocomposites from VSM Characterization

CONCLUSION

The BZT-BFO nanocomposite synthesized in this study shows a unique combination of reduced crystallite size, dense microstructure, thermal stability, and enhanced ferroelectric properties. These characteristics directly support its potential integration into next-generation flexible and wearable electronic systems.

Flexible piezoelectric–ferroelectric sensors for physiological monitoring (heart rate, respiration, gait analysis)

The strong remanent polarization and low coercive field of BZTBFO enable highly sensitive detection of minute biomechanical signals such as pulse waves, thoracic expansion during breathing, and foot-strike forces during gait. Its nanoscale grain structure allows stable signal output even under repeated bending, making it ideal for continuous physiological monitoring [3].

Wearable pressure and strain sensors embedded in soft textiles

The composite's enhanced dielectric response allows precise transduction of small pressure or strain variations when integrated into woven or knitted fabrics. Its mechanical compliance ensures that the sensor conforms to body movements without cracking, supporting comfortable, long-term wearability[6].

Self-powered flexible devices based on piezoelectric energy harvesting

BZTBFO's high polarization and piezoelectric activity enable efficient conversion of everyday mechanical motion—walking, joint movements, or fabric deformation—into electrical energy. This supports the development of battery-free wearable

systems that power low-consumption health and motion-tracking modules [3].

Smart e-skins require highly responsive, low-power switching behavior

The material's low coercivity facilitates fast, low-energy switching of ferroelectric domains, a key requirement for electronic skins that mimic tactile sensing. Its multiferroic behavior allows multifunctional sensing (pressure, vibration, magnetic cues) within a single flexible layer [1].

Multiferroic components in bendable memory elements for wearable electronics

The combined ferroelectric and magnetic ordering in BZTBFO enables the realization of nonvolatile memory elements that retain information even when bent or stretched. Such stable switching properties make the composite well-suited for next-generation flexible memory arrays and logic circuits [1,5].

LIMITATIONS

The synthesis approach using low-temperature sintering may introduce phase impurities and incomplete grain growth. Trade-offs such as reduced phase purity in BFO at 800°C and potential volatilization effects should be considered.

REFERENCES

1. Spaldin NA, Cheong SW, Ramesh R. Multiferroics: Past, present, and future. *Journal of Physics: Condensed Matter*. 2010;22(16):164203.
2. Ismail MM, Ali SM, Ahmed ZS, Cao WQ. Structure and morphology of nanocrystalline BZT powders prepared using hydrothermal method. *Materials Science and Engineering B*. 2018;229:120–128.
3. Jha PA, Jha PK, Jha AK, Dwivedi RK. Dielectric behavior of (1-x) BaZrTiO₃–(x) BiFeO₃ ceramics. *Ceramics International*. 2020;46(8):10345–10353.
4. Selbach SM, Einarsrud MA, Tybell T, Grande T. Synthesis of BiFeO₃ by wet chemical methods. *Chemistry of Materials*. 2007;19(26):6470–6475.
5. Zhang ST, Zhang Y, Luo ZL, et al. Multiferroic properties of Bi_{0.8}La_{0.2}FeO₃/CoFe₂O₄ multilayer thin films. *Applied Physics Letters*. 2005;87(20):202505.
6. TIFAC. Nanocomposites – technology trends and application potential. *TIFAC Reports*. 2016.
7. Chourasia R, Shrivastava OP. Structural, electrical and microstructural characterization of manganese-doped barium zirconate titanate ceramics. *Ceramics International*. 2015;41(2):2673–2680.
8. Zhang YR, Motohashi T, Masubuchi Y, Kikkawa S. Sintering and dielectric properties of perovskite SrTaO₂N ceramics. *Journal of the American Ceramic Society*. 2022;105(5):2569–2578.